Available online at www.sciencedirect.com
ScienceDirect
Thin Solid Films 515 (2007) 5808–5813
www.elsevier.com/locate/tsf

In situ deposition of cadmium chloride films using MOCVD for CdTe solar cells

V. Barrioz *, S.J.C. Irvine, E.W. Jones, R.L. Rowlands, D.A. Lamb

School of Chemistry, University of Wales, Bangor, Deiniol Road, Bangor, Gwynedd, LL57 2UW, Wales, United Kingdom

Available online 30 January 2007

Abstract

This paper reports on the first deposition of cadmium chloride ($CdCl_2$) films by metal organic chemical vapour deposition (MOCVD). As the p–n junction can be deposited by MOCVD, the *in situ* $CdCl_2$ treatment of the device allows for containment of the whole process. MOCVD allows a high level of control over material properties and excellent repeatability. Deposition of $CdCl_2$, on glass and silicon, at different II:VII precursor ratios and substrate temperatures are reported. The precursors used are dimethylcadmium and tertiarybutylchloride or *n*-hexylchloride, respectively for the cadmium and chlorine species. Results are presented on the surface morphology and layer structure. $CdCl_2$ was in its hydrate form once exposed to ambient air. Preliminary results on the effects of *in situ* $CdCl_2$ treatment on MOCVD CdS/CdTe:As devices are reported and compared with untreated devices, using current–voltage characterisation. The $CdCl_2$ treatment successfully resulted in MOCVD devices having open-circuit voltage higher than 600 mV and fill factor above 50%.

Keywords: Cadmium chloride; MOCVD; Cadmium telluride; Photovoltaic

1. Introduction

Cadmium telluride (CdTe) is one of the contender materials for thin film photovoltaic (PV) solar cells with a near optimum direct band gap of 1.5 eV and low cost of raw materials. The p–n heterojunction is conventionally formed using cadmium sulphide (CdS) as a window layer (n-type) and CdTe as the absorber layer (p-type). As a consequence, both layers are polycrystalline with grains of the order of the layer thickness. To reduce the photocurrent losses by carrier recombination at the grain boundaries [1,2], a thin $CdCl_2$ layer is deposited on the CdTe layer using physical vapour deposition [3,4], or by spraying aqueous solution [5], followed by an annealing of the device at around 400 °C under nitrogen or oxygen. Alternatively, vapour transport of chlorine (Cl) or cadmium chloride during annealing can also be used [6,7]. This $CdCl_2$ treatment has the effect of passivating the grain boundaries and may provide a flux to promote lateral grain growth (i.e. depending on the initial grain size) [1–8].

The current dilemma of the overall p–n junction process and activation is that each step is carried out in a different environment with potential for process variability. Typically, the process steps are as follow: (i) the CdS is deposited at low temperature by chemical bath deposition (CBD) before being annealed; (ii) the CdTe is then deposited at high temperature (~500 °C) by closed space sublimation (CSS); (iii) the $CdCl_2$ treatment is then applied by one of the methods described above. The ideal solution would be the containment of the overall device production within the same process. Metal organic chemical vapour deposition (MOCVD) can, in principle, achieve this goal but the critical step of depositing $CdCl_2$ by MOCVD has not previously been demonstrated.

MOCVD has been extensively used for optoelectronic devices such as cadmium mercury telluride (CMT) infrared detectors [9], where the fine control of electrical, physical and chemical properties of the layers is paramount. In 1990, Chu et al. [10] showed that CdTe, grown by MOCVD, could be used for the photovoltaic application. Good photovoltaic conversion efficiencies have been obtained using MOCVD for CdS while using CSS for CdTe [11]. The potential for depositing the full CdTe/CdS junction by MOCVD using alkyl precursors was first reported in 1998 [12]. Since then, improved p-type activation of

* Corresponding author. Tel.: +44 1248 382 235; fax: +44 1248 370 528.
E-mail address: v.barrioz@bangor.ac.uk (V. Barrioz).

0040-6090/$ - see front matter © 2006 Elsevier B.V. All rights reserved.
doi:10.1016/j.tsf.2006.12.043

the CdTe absorber layer has been achieved using arsenic (As) doping without $CdCl_2$ treatment [13].

In this paper, the novel deposition of $CdCl_2$, on glass and silicon substrates, by atmospheric pressure MOCVD and subsequent *in situ* annealing, on CdTe PV cells, is investigated and characterised using scanning electron microscopy (SEM), X-ray diffraction (XRD) and *in situ* interferometry. Preliminary current–voltage (*J–V*) characteristics of an all-in-one MOCVD process for activated p–n junctions, using the *in situ* $CdCl_2$ treatment, are also reported in this paper and compared with untreated CdTe solar cells.

2. Experimental

2.1. MOCVD of $CdCl_2$

The deposition of $CdCl_2$ was carried out in a horizontal MOCVD reactor at atmospheric pressure with hydrogen as a carrier gas. Dimethylcadmium (DMCd) and tertiarybutylchloride (tBuCl) or *n*-hexylchloride (*n*-HexCl) alkyl precursors were used, respectively, for the cadmium (Cd) and chlorine species. The calibration of the partial pressure of the precursors was carried out using an Epison II from Thomas Swan. The partial pressure of DMCd was kept constant at 28.4 Pa, when using tBuCl, and at 20.3 Pa while using *n*-HexCl. The II:VII precursor ratio was either Cl rich (0.29 or 0.45) while using tBuCl or Cd rich (2) when using *n*-HexCl. Using the *n*-HexCl, it was not possible to achieve a Cl rich precursor ratio due to the flow limitation from the mass flow controllers used, combined with the low saturated vapour pressure of *n*-HexCl. The metal organic precursors were introduced inside the reactor for 50 min for each run. $CdCl_2$ was deposited on both glass substrates and silicon wafers 3° off (111). The substrates were placed on a non-rotating graphite susceptor. The stable substrate temperature (T_s) during deposition was achieved using a graphite resistive heater able to reach 600 °C.

2.2. Analytical apparatus and techniques

The deposition of all layers was monitored using an *in situ* triple-wavelength reflectometer operating normal to the substrate surface. The layer thickness, deposition rate and material properties can be determined using the Fabry–Perot interference equation [14]. The use of different laser wavelengths (i.e. 532 nm, 635 nm, and 980 nm) allows different band gap materials to be monitored without losing the interferometer oscillations.

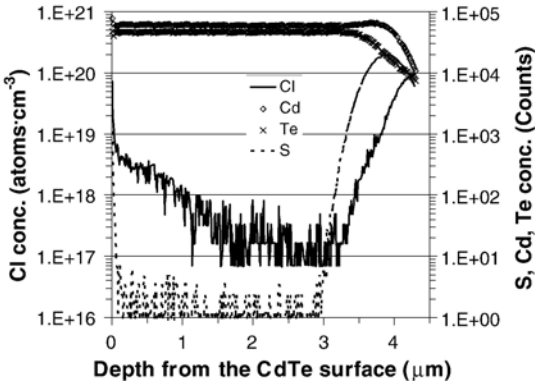

Fig. 1. SIMS depth profile of a CdTe/CdS structure after Cd–Cl post-treatment using *n*-HexCl and DMCd as precursors. There is evidence of chlorine diffusion into the CdTe layer.

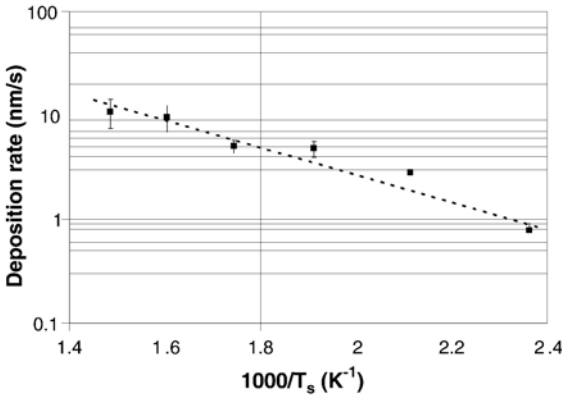

Fig. 2. The Arrhenius graph of the deposition rate of $CdCl_2$ using DMCd and tBuCl as precursors in a total gas flow of 3500 cm^3 min^{-1}. The partial pressure of DMCd was 28.4 Pa with a II:VII precursor ratio of 0.29. The solid squares represent the experimental data. The line is fitted to determine the activation energy (E_a) of the reaction.

The SEM, used to examine surface morphology, was a S-520 from Hitachi. The samples studied were pre-coated with a sputtered thin gold layer to provide electron conduction from the sample surface to the stud. Using cross-sectional mounted samples, it was also possible to measure the thickness of the layers and consequently deduce their deposition rates. Three cross-sectional pictures per sample were used to calculate the average value of the layer thicknesses and their standard deviations, using 10 data points each time. The error bars in the graphs are the calculated standard deviation values.

The powder XRD was a PW3040/60 X'Pert PRO from Philips. Due to the hygroscopic nature of $CdCl_2$, the XRD spectra were completed within 5 h of the sample being open to ambient air. The X'pert HighScore software was used to determine the indexing of the $CdCl_2$ layers.

The *J–V* characterisation was carried out with a set of 4 halogen lamps to provide a constant 100 mW cm^{-2} light power density over a 2.5 cm^2 activated cell area, measured using a broadband thermopile power meter from Melles Griot. *J–V* characteristics, for 30 different devices, from this setup were compared with those of a solar simulator from ORIEL (300 W), calibrated for an AM 1.5 global spectrum using a calibrated cell, at the University of Durham. It was found that cell efficiencies were on average 63% lower than for our setup with the highest difference coming from the J_{sc}. This difference was corroborated by a comparison of the different spectral irradiance of the halogen lamps with an AM 1.5 spectrum, taking into account the spectral range for high quantum efficiency of a CdTe solar cell. A Keithley 2400 source/meter was used to sweep the voltage and measure the current density. The device PV characteristics were obtained from these curves. After the *in situ* $CdCl_2$ treatment, a 5 second bromine–methanol etch, with

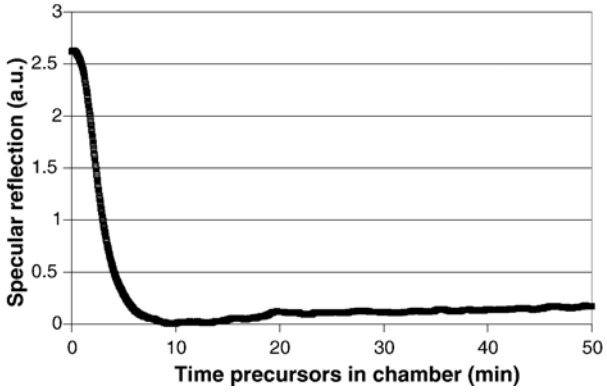

Fig. 3. Specular reflection, from the 635 nm laser wavelength of the *in situ* reflectometer, during the deposition of a $CdCl_2$ layer at 300 °C. The II:VII precursor ratio was 0.45 and the total gas flow was 2500 cm^3 min^{-1}. The specular reflection is rapidly lost without any visible interference oscillations characteristic of a Volmer–Weber mechanism. After 13 min, some specular reflection recovery occurs associated with the coalescence of the islands with growing layer thickness.

0.26% bromine solution, was used on the CdTe:As surface prior to the deposition of either 2.5 mm^2 or 26.5 mm^2 gold back contacts.

3. Results and discussion

3.1. n-HexCl for the deposition of $CdCl_2$ layers

In a previous study [13], the use of DMCd and *n*-HexCl was explored to deposit a $CdCl_2$ cap layer on the arsenic doped cadmium telluride (CdTe:As). The results appeared beneficial both from the Taguchi result, improving the photocurrent collection, and secondary ion mass spectrometry (SIMS) analysis showing the presence of Cl within the CdTe layer. Consequently an attempt was made to deposit this layer directly onto glass to monitor the deposition rate. However, after failing to obtain a measurable amounts of $CdCl_2$ at a substrate temperature of 350 °C and 450 °C, it was concluded that the *n*-HexCl was either too

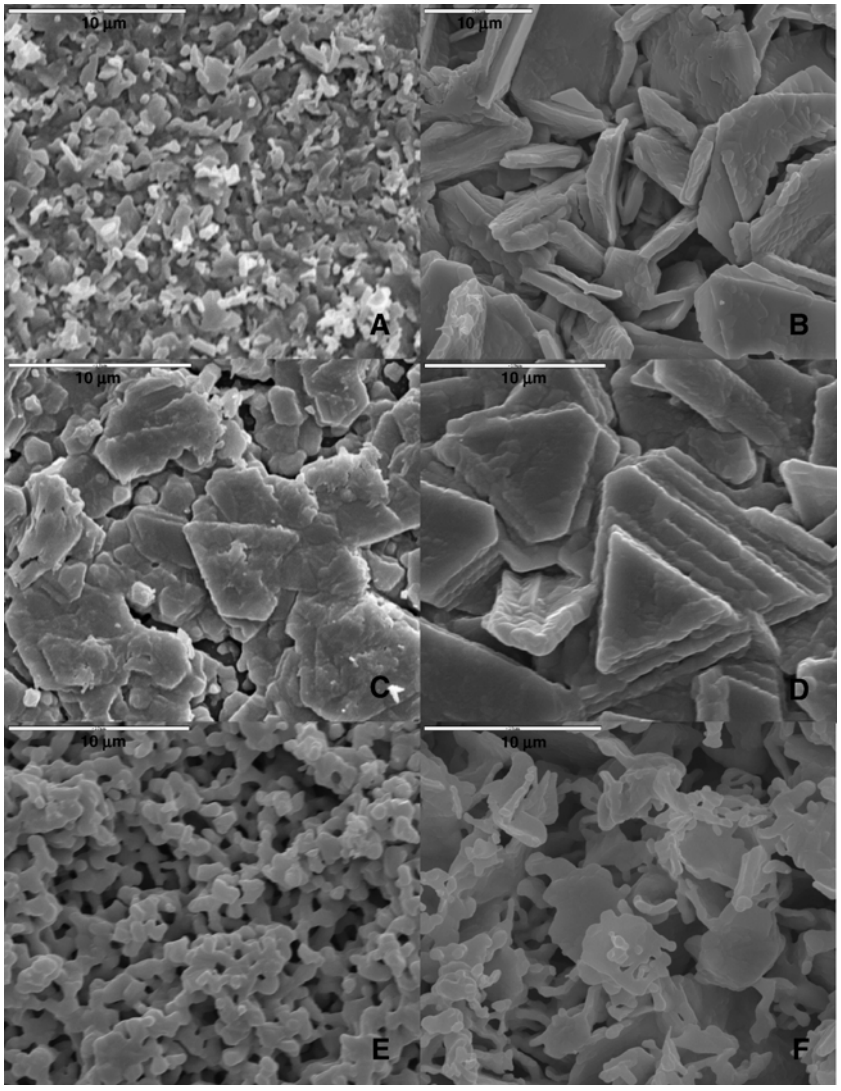

Fig. 4. SEM micrographs of $CdCl_2$ layers deposited on glass by MOCVD. The fixed parameters were: deposition time of 50 min, total gas flow of 3500 cm^3 min^{-1}, DMCd partial pressure of 28.4 Pa and II:VII precursor ratio of 0.29. The substrate temperatures during deposition were (A) 150 °C, (B) 200 °C, (C) 250 °C, (D) 300 °C, (E) 350 °C, and (F) 400 °C. The markers are all 10 µm.

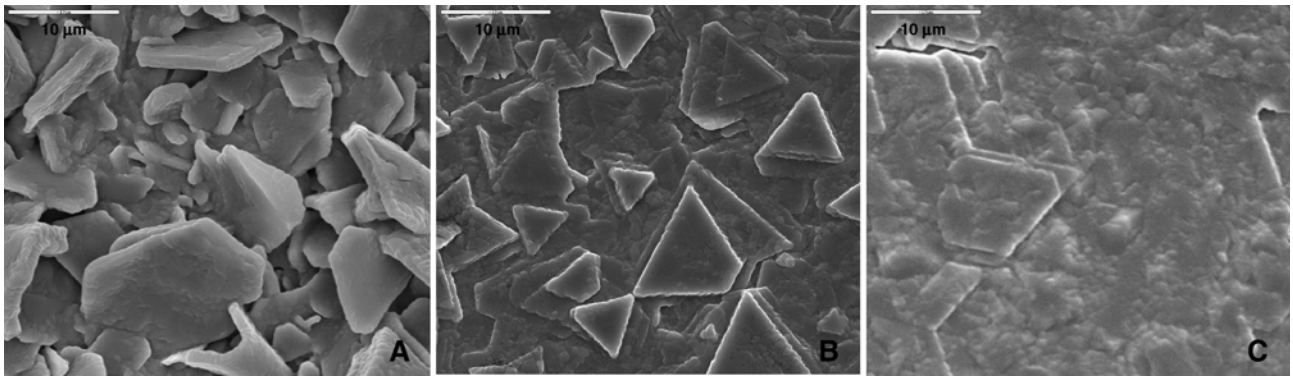

Fig. 5. SEM micrographs of $CdCl_2$ layers deposited on silicon (111) by MOCVD. The fixed parameters were: deposition time of 50 min, total gas flow of 3500 cm^3 min^{-1}, DMCd partial pressure of 28.4 Pa and II:VII precursor ratio of 0.29. The substrate temperatures during deposition were (A) 200 °C, (B) 300 °C, and (C) 350 °C. The markers are all 10 µm.

stable at these temperatures or the partial pressure was too low. However, from the SIMS depth profile of CdTe/CdS structures, as shown in Fig. 1, there was evidence of some surface reaction to yield Cl concentrations of up to 5×10^{18} atoms cm^{-3} in the CdTe layer, which provided some encouragement. Attention was then switched to tBuCl which had a higher saturated vapour pressure of 7.7 kPa at −5 °C.

3.2. Growth of $CdCl_2$ layers as a function of T_s

The substrate temperature is one of the dominant factors that can influence the properties and structure of a layer. For this study the II:VII precursor ratio was fixed at 0.29 and the total gas flow was constant at 3500 cm^3 min^{-1}, while T_s was varied from 150 °C to 400 °C with 50 °C increments. The deposition rate as a function of the substrate temperature is shown as an Arrhenius plot in Fig. 2. In this temperature region, the plot is linear, so that the reaction is kinetically limited; hence the growth rate is not limited by precursor supply rate. The activation energy (E_a) of the pyrolytic deposition of $CdCl_2$, from DMCd and tBuCl, was determined, from the slope, to be 25 kJ mol^{-1}.

The deposition rates were solely determined from the SEM cross-section micrographs as the *in situ* reflectometer, monitoring the layer deposition on the silicon wafer, showed an exponential loss of specular reflection, without any Fabry–Perot oscillations, due to surface roughening, as shown in Fig. 3. The absence of interference oscillations for most of the growth experiments indicated that the $CdCl_2$ layers grew by a Volmer–Weber mechanism.

The surface microstructure of these $CdCl_2$ layers was highly dependent on T_s during deposition. The melting point of $CdCl_2$ is 568 °C and its vapour pressure at 656 °C is 13.3 kPa. The change in the surface morphology as a function of substrate temperature is shown on the SEM micrographs of Fig. 4. It is worth pointing out that the layer thickness increases with increasing substrate temperature as the deposition time was kept constant. For $T_s<200$ °C, small grains with an average size of 760 nm evenly cover the surface but without order due to a lack of kinetic energy at such low substrate temperatures. For 200 °C $<T_s<$ 300 °C, more coalescence of the grains arise, with a larger size of 950 nm, agglomerating into distinct islands. This

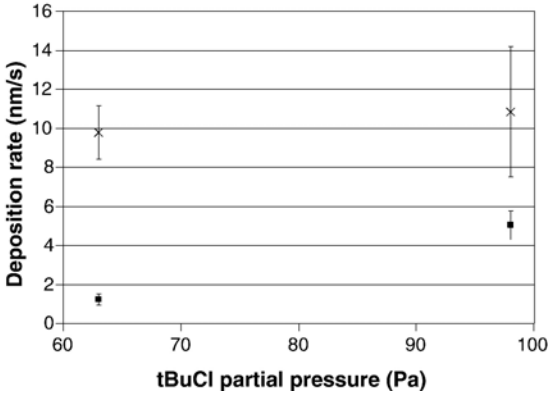

Fig. 6. Plot of the deposition rate as a function of tBuCl partial pressure. The fixed parameters were: deposition time of 50 min, total gas flow of 3500 cm^3 min^{-1} and DMCd partial pressure of 28.4 Pa. Squares and crosses indicate substrate temperature of 300 °C and 400 °C respectively. The II:VII precursor ratios were 0.29 and 0.45 for tBuCl partial pressures of 98 and 63 Pa respectively.

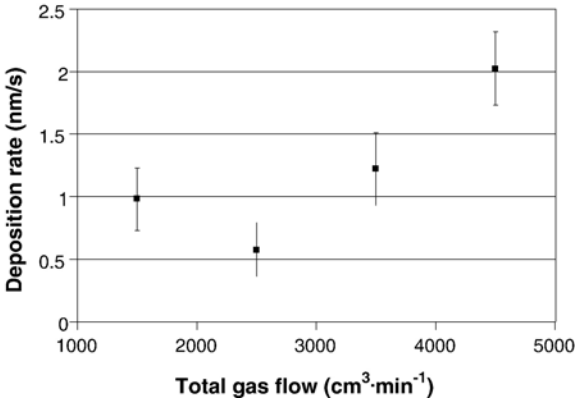

Fig. 7. Graph of the deposition rate as a function of total gas flow in the reactor. The II:VII precursor ratio was fixed at 0.45 with a DMCd partial pressure of 28.4 Pa while T_s was 300 °C.

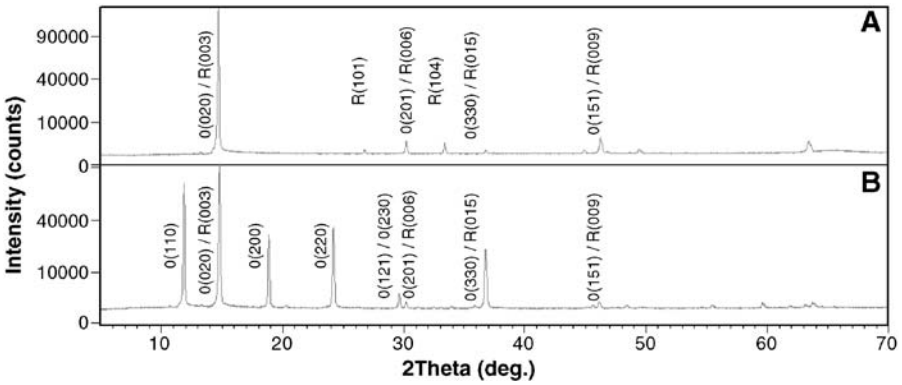

Fig. 8. XRD spectra of $CdCl_2$ deposited at (A) 250 °C and (B) 300 °C, on silicon (111). The prefix letters R and O, in front of the Miller indices, indicate the respective rhombohedral $CdCl_2$ and orthorhombic $CdCl_2$:H_2O crystal lattices, to which the peaks can be attributed.

deposition mechanism, confirmed by the *in situ* reflectometer, is characteristic of the Volmer–Weber growth where only 3D growth takes place and the islands eventually coalesce to form a continuous layer. For the layer grown at 300 °C, equilateral triangle shaped islands, where their sides are longer than 7 μm, indicate a crystallographic preferred orientation with 3-fold symmetry. The grain size reduces to 760 nm for $T_s > 300$ °C. This behaviour can be associated with re-evaporation of the $CdCl_2$ given the high vapour pressure. On silicon wafers, a $CdCl_2$ layer was only present for 200 °C $< T_s <$ 350 °C, as shown in Fig. 5. Uniform 2D coverage is found at $T_s > 250$ °C. At $T_s = 350$ °C, the $CdCl_2$ layer structure is porous on glass and compact on silicon, this would indicate that the surface free energy for nucleation is lower on silicon than glass substrates.

3.3. Influence of the II:VII precursor ratio

Two tBuCl rich II:VII precursor ratios, namely 0.29 and 0.45, were investigated for two substrate temperatures of 300 °C and 400 °C. The effect on deposition rate as a function of the tBuCl partial pressure is shown in Fig. 6. The partial pressure of DMCd and total gas flow were kept constant. The concentration of tBuCl in the gas stream has a super-linear effect on the deposition rate and hence on the formation of $CdCl_2$ at the surface of the substrate for 300 °C. A saturation level in deposition rate, at $T_s = 400$ °C, would indicate that in this regime re-evaporation is increasing, supported by the porous surface morphology observed in Fig. 4(F). However, with these preliminary experiments, it appears as if the increase in tBuCl supply is assisting in the decomposition of the DMCd precursor at lower temperatures where the pyrolysis rate of DMCd is slow.

3.4. Effect of varying the total gas flow

The total gas flow was varied from 1500 to 4500 cm^3 min^{-1} to look at the potential limitation on mass transport in the gas stream. It is also an effective way to change the deposition rate while keeping the DMCd partial pressure and II:VII precursor ratio constant. Fig. 7 illustrates the variation of deposition rate as a function of the total gas flow. The saturation observed in deposition rate for total flows lower than 2500 cm^3 min^{-1} would suggest a limitation caused by depletion of the precursors for a II:VII precursor ratio of 0.45. For higher total gas flows, the deposition rate increases linearly with no apparent plateau. At 1500 cm^3 min^{-1}, some oscillations were observed with the *in situ* reflectometer before losing the specular reflection. Both the green and red interferograms were analysed, using the Fabry–Perot interference equation. The results gave a deposition rate of 0.7 nm/s, a refractive index (n) of 1.05 and an absorption coefficient (k) of 0.02. Within experimental errors, the deposition rate given by the *in situ* reflectometer and the SEM were in agreement.

3.5. The crystal structure of $CdCl_2$

Using the number of counts from the XRD spectra, the best crystallinity of the $CdCl_2$ layer was for 200 °C $< T_s <$ 300 °C. However there are two distinct crystalline structures within a difference of just 50 °C in deposition temperature, as observed in Fig. 8. The layers grown at 250 °C showed a dominance of the $CdCl_2$ rhombohedral crystal lattice, with a (003) preferred orientation as well as the presence of the (101) and (104) unambiguous peaks, both when deposited on glass and silicon. At a substrate temperature of 300 °C, the (110), (200), and (220) peaks, specific to the orthorhombic hydrate form ($CdCl_2$:H_2O), are clearly visible. The dewpoint under hydrogen was < −80 °C, consequently hydration of the hygroscopic $CdCl_2$ is unlikely

Table 1
List of J–V characteristics of MOCVD photovoltaic CdTe solar cell both *in situ* $CdCl_2$ treated and untreated

Grown cell structure	Contact area (mm^2)	η (corrected for AM 1.5) (%)	FF (%)	J_{sc} (corrected for AM 1.5) (mA cm^{-2})	V_{oc} (mV)
CdS/CdTe: As	2.5	3	47.5	12.1	510
CdS/CdTe: As/$CdCl_2$	2.5	7.4	51.8	23.9	600
CdS/CdTe: As/$CdCl_2$	2.5 (scribed)	5.6	49.9	18.8	600
CdS/CdTe: As/$CdCl_2$	26.5	6.3	50.7	20.7	600

The measurements were carried out under a 100 mW cm^{-2} illumination using halogen lamps and corrected for AM 1.5.

inside the reactor. Therefore it is proposed that $CdCl_2$ layers are deposited as a rhombohedral crystal lattice. Only once opened to ambient air, the orthorhombic $CdCl_2$:H_2O compound forms and the extent of transformation will depend on the microstructure of the deposited layer. Furthermore, due to the $CdCl_2$ layer thickness being >2 μm, the surface hydrate would be screening the underlying rhombohedral structures. More XRD would be needed to investigate the hydrate transformation of the compound.

3.6. Comparison between treated and non-treated PV cells

The deposition of PV structures, inside the same horizontal MOCVD reactor, was detailed elsewhere [15]. The CdS layer was 240 nm thick and deposited at a substrate temperature of 315 °C. The CdTe:As layer was deposited at a substrate temperature of 390 °C. The layer thickness was 4–5 μm. The uniform concentration of arsenic throughout the cadmium telluride layer thickness was 2×10^{18} atoms cm^{-3}. Without the *in situ* $CdCl_2$ deposition, the cell efficiency on a small area device was 3% (AM 1.5), well below that expected of a CdTe cell. However, without the As doping, the structure is inactive. The $CdCl_2$, was deposited at a substrate temperature of 300 °C, and estimated to be 450 nm thick. The annealing treatment of the full device was carried out at 400 °C for 10 min under a flow of hydrogen. All these process steps were carried out in a single chamber, as a continuous process. The *in situ* anneal temperature was kept to a minimum to avoid other diffusion effects, being only 10 °C above the CdTe growth temperature. Table 1 summarises the *J–V* characteristics of both $CdCl_2$ treated and untreated cells. For the *in situ* $CdCl_2$ treated cells, cell efficiencies have more than doubled both on small and large area contacts with an open-circuit voltage (V_{oc}) of 600 mV and a fill factor (FF) above 50% and highest AM 1.5 corrected J_{sc} of 23.9 mA cm^{-2}. To check for the effects of lateral collection on the small area devices, larger contacts were made and a small contact was scribed around its perimeter. The scribing appears to have damaged the edge of the device and can be considered as a lower limit. The larger area device *J–V* characteristics are probably closer to the true photo-response of the cell.

4. Conclusion

The first reported deposition of $CdCl_2$ by MOCVD, using DMCd and tBuCl has been described in this paper. The hygroscopic nature of this compound has been confirmed and emphasises the potential need for a contained process such as MOCVD to avoid variability of oxygen inclusion. The crystallinity and surface coverage of $CdCl_2$ layers are best for 200 °C < T_s < 300 °C. More work will be needed to optimise the parameters used to deposit the $CdCl_2$ layer for PV cell activation together with the anneal treatment. Preliminary results on a CdS/CdTe:As/$CdCl_2$ activated cell showed a net improvement of the overall *J–V* characteristics compared to a standard CdS/CdTe:As photovoltaic cell, where the cell efficiency has more than doubled and reasonable V_{oc} and FF were achieved (i.e. V_{oc} = 600 mV and FF ≥ 50%) with highest J_{sc} of 23.9 mA cm^{-2}. This new process offers the potential for better control over the chlorination step, compared to *ex situ* treatment.

Acknowledgements

The authors would like to acknowledge EPSRC for their financial support on the PV SuperGen project (PV Materials for the 21st Century). Epichem Ltd is acknowledged for their support with organometallic precursors. Prof. Ken Durose is greatly thanked for allowing the use of the solar simulator in his laboratory. Drs Hamid Kheyrandish and Simon Romani are acknowledged for the SIMS analysis. The authors also wish to thank Steve Jones for operation of the XRD under tight deadlines.

References

[1] V.G. Karpov, D. Shvydka, Y. Roussillon, in: W. Shafarman, T. Gessert, S. Niki, S. Siebentritt (Eds.), Thin-Film Compound Semiconductor Photovoltaics, San Francisco, U.S.A., March 28–April 1, 2005, Materials Research Society Symposium Proceedings, vol. 865, 2005, p. 307.
[2] J.R. Sites, J.E. Granata, J.F. Hiltner, Sol. Energy Mater. Sol. Cells 55 (1998) 43.
[3] A. Fischer, C. Narayanswamy, D.S. Grecu, E. Bykov, S.A. Nance, U.N. Jayamaha, G. Contreras-Puente, A.D. Compaan, M.A. Stan, A. Mason, 25th IEEE Photovoltaic Specialists Conference, Washington, U.S.A., May 13–17, 1996, p. 921.
[4] G. Zoppi, K. Durose, S.J.C. Irvine, V. Barrioz, in: W. Hoffmann, J.-L. Bal, H. Ossenbrink, W. Palz, P. Helm (Eds.), 19th European Photovoltaic Solar Energy Conference Proceedings, Paris, France, June 7–11, 2004, p. 1921.
[5] T. Aramoto, F. Adurodija, Y. Nishiyama, T. Arita, A. Hanafusa, K. Omura, A. Morita, Sol. Energy Mater. Sol. Cells 75 (2003) 211.
[6] B.E. McCandless, K.D. Dobson, Sol. Energy 77 (2004) 839.
[7] C.S. Ferekides, U. Basasubramanian, R. Mamazza, V. Viswanathan, H. Zhao, D.L. Morel, Sol. Energy 77 (2004) 823.
[8] S. Lalitha, R. Sathyamoorthy, S. Senthilarasu, A. Subbarayan, Sol. Energy Mater. Sol. Cells 90 (2006) 694.
[9] L.O. Bubulac, S.J.C. Irvine, E.R. Gertner, J. Bajaj, W.P. Lin, R. Zucca, Semicond. Sci. Technol 8 (1993) S270.
[10] T.L. Chu, S.S. Chu, C. Ferekides, J. Britt, C.Q. Wu, Proceedings of the 2nd International Conference on Electronic Materials, Newark, U.S.A., September 17–19, 1990, p. 345.
[11] M. Tsuji, T. Aramato, H. Ohyama, T. Hibino, K. Omura, J. Cryst. Growth 214/215 (2000) 1142.
[12] R.A. Berrigan, N. Maung, S.J.C. Irvine, D.J. Cole-Hamilton, D. Ellis, J. Cryst. Growth 195 (1998) 718.
[13] V. Barrioz, R. Rowlands, S.J.C. Irvine, in: W. Palz, H. Ossenbrink, P. Helm (Eds.), 20th European Photovoltaic Solar Energy Conference Proceedings, Barcelona, Spain, June 6–10, 2005, p. 1918.
[14] S.J.C. Irvine, A. Hartley, A. Stafford, J. Cryst. Growth 221 (2000) 117.
[15] V. Barrioz, R.L. Rowlands, E.W. Jones, S.J.C. Irvine, G. Zoppi, K. Durose, in: W. Shafarman, T. Gessert, S. Niki, S. Siebentritt (Eds.), Thin-Film Compound Semiconductor Photovoltaics, San Francisco, U.S.A., March 28–April 1, 2005, Materials Research Society Symposium Proceedings, vol. 865, 2005, p. 67.